

Research Article

Autothermal reforming of palm empty fruit bunch bio-oil: thermodynamic modelling

Lifita N. Tande * and Valerie Dupont

Energy Research Institute, School of Chemical and Process Engineering, The University of Leeds, LS2 9JT, UK

* **Correspondence:** Email: pmlnt@leeds.ac.uk; Tel: +44 (0)-113-343-2503;
Fax: +44 (0)-113-246-7310

Abstract: This work focuses on thermodynamic analysis of the autothermal reforming of palm empty fruit bunch (PEFB) bio-oil for the production of hydrogen and syngas. PEFB bio-oil composition was simulated using bio-oil surrogates generated from a mixture of acetic acid, phenol, levoglucosan, palmitic acid and furfural. A sensitivity analysis revealed that the hydrogen and syngas yields were not sensitive to actual bio-oil composition, but were determined by a good match of molar elemental composition between real bio-oil and surrogate mixture. The maximum hydrogen yield obtained under constant reaction enthalpy and pressure was about 12 wt% at S/C = 1 and increased to about 18 wt% at S/C = 4; both yields occurring at equivalence ratio Φ of 0.31. The possibility of generating syngas with varying H₂ and CO content using autothermal reforming was analysed and application of this process to fuel cells and Fischer-Tropsch synthesis is discussed. Using a novel simple modelling methodology, reaction mechanisms were proposed which were able to account for equilibrium product distribution. It was evident that different combinations of reactions could be used to obtain the same equilibrium product concentrations. One proposed reaction mechanism, referred to as the ‘partial oxidation based mechanism’ involved the partial oxidation reaction of the bio-oil to produce hydrogen, with the extent of steam reforming and water gas shift reactions varying depending on the amount of oxygen used. Another proposed mechanism, referred to as the ‘complete oxidation based mechanism’ was represented by thermal decomposition of about 30% of bio-oil and hydrogen production obtained by decomposition, steam reforming, water gas shift and carbon gasification reactions. The importance of these mechanisms in assisting in the eventual choice of catalyst to be used in a real ATR of PEFB bio-oil process was discussed.

Keywords: Bio-oil; autothermal reforming; thermodynamic analysis; reaction mechanism; hydrogen;

1. Introduction

The need to find alternative sources of energy to substitute fossil fuel has gained a lot of attention with increased awareness in the role greenhouse gases play in global warming [1]. These greenhouse gases, together with other pollutant gases, are produced during the combustion of fossil fuel and include CO₂, SO₂ and NO_x [2]. Biomass, defined as biological material obtained from a living or recently living organism, is being considered as a substitute to fossil fuel since it is abundant and can be readily accessed and processed sustainably. Though the combustion of biomass/biofuel generates CO₂, it is considered a near-neutral carbon process since the CO₂ released during combustion is in part the same CO₂ absorbed by plants when synthesizing carbohydrates during photosynthesis [3]. However, fossil CO₂ emissions may occur during soil conditioning by use of synthetic fertilizers, and also during transportation and storage when using conventional vehicles and equipment for biomass production and processing. One other major drawback with the use of fossil fuel is that it is a finite source of energy and existing world reserves are known to be depleting fast as a result of increase in world demand [2-5]. Due to its complex organic nature, biomass can serve as feedstock, either directly or indirectly after processing, for the production of multiple bio-based chemical products [6,7]. Biomass can be valorised by thermochemical conversion into bio-oil which is a dark brown, polar, high-density and viscous organic liquid containing a complex mixture of oxygenated compounds such as sugars, carboxylic acids, phenols, esters, ketones, aldehydes and benzenoids [8-10]. Palm empty fruit bunch (PEFB) is obtained after oil extraction at palm oil mills. It is estimated that for every tonne (t) of palm oil produced from a fresh fruit bunch, approximately 1 t of PEFB is produced [11].

Bio-oil can be produced by fast/flash pyrolysis, slow pyrolysis and solvolysis of solid biomass feedstock [12]. Pyrolysis is the thermal decomposition of biomass in the absence of oxygen (or in the presence of a limited amount of oxygen) at temperatures ranging from 400 °C to 600 °C [13]. Many studies have been carried out to understand the thermochemical conversion of biomass into bio-oil (also called pyrolysis oil) with authors focusing on process parameters such as pre-treatment of biomass, particle size of feedstock, reaction temperature, reactor type, choice of catalyst and reaction time. Depending on process conditions and the presence or absence of catalyst, bio-oil yield from PEFB can range from 30–70 wt% of the solid feedstock, with non-condensable gases and solid char formed as co-products [14-17]. In a study carried out by Mantilla et al. [9], PEFB pyrolysis experiments were conducted in a fixed-bed reactor at temperatures 460–600 °C, gas residence time 16–80 s and particle size <0.5 mm, as well as 0.5–1.4 mm. The maximum yield of bio-oil of 48.4 wt% was obtained at a temperature 540 °C, gas residence time of 31 s and particle size <0.5 mm. Their study concluded that temperature was the most significant parameter, of the three considered, in determining the bio-oil yield. Abdullah et al. [18], studied the fast pyrolysis of PEFB using a fluidised bed system for which the reactor temperature was varied from 400 to 600 °C, the residence time between 0.79–1.32 s, and particle size diameters (with corresponding ash content) were <150 µm (8.49%), 150–250 µm (7.46%), 250–300 µm (6.70%) and 355–500 µm (4.83%). They obtained optimum bio-oil yields at a pyrolysis temperature of 450 °C, retention time of 1.02 s and for the particle size 355–500 µm with the lowest ash content. The somewhat high ash content of PEFB

(rich in potassium) particularly reduces the yield in bio-oil resulting in the need for pre-treatment options before pyrolysis. Abdullah & Gerhauser [14] were able to demonstrate that by washing PEFB feedstock with distilled water before pyrolysis, the yield in bio-oil (organic phase) obtained rose to 61.3 wt% which was significantly higher than that obtained for the unwashed PEFB of 34.7 wt%. Solvolysis, or hydrothermal liquefaction, is the use of highly pressurised solvent (pressure > critical pressure of solvent) such as water, methanol, ethanol or mixture of water and organic solvent to cause the decomposition of biomass to yield bio-oil at mild temperatures, usually < 400 °C [11,19]. A few studies have been carried out to determine the influence of different solvent and catalyst on the production of bio-oil by solvolysis of PEFB. Akhtar et al. [20], investigated the effect of different catalysts such as NaOH, KOH and K₂CO₃ on PEFB solvolysis with water as solvent. The highest bio-oil yield of about 67 wt% was obtained with K₂CO₃ catalyst with a concentration of 1 M. Table 1 presents a summary of some selected PEFB bio-oil composition published by various authors.

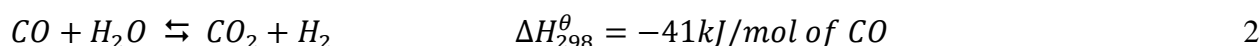
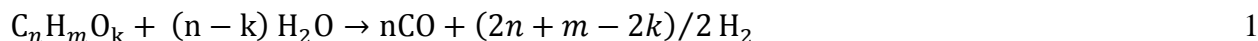
Table 1. Summary of PEFB bio-oil composition obtained in literature.

	[15]	[16]	[18]	[21]	[22]	[23]
Pyrolysis temperature (°C)		480		500		600
Reactor	Fluidised	Fluidised		Fluidised		Kiln
Moisture	7.9	0	7.90	18.74	24.30	5.2
Proximate analysis (%)						
Volatile matter					84.3	
Fixed carbon					11.3	
Ash				0.65	2.43	0.1
Solids						
Ultimate analysis (%)						
C	69.35	58.65	69.35	49.80	45.23	68.26
H	9.61	7.02	9.61	7.98	6.53	8.02
O	20.02	30.14	20.02	40.29	47.03	21.57
N	0.74	2.74	0.74	1.93	8.5×10^{-3}	2.02
S		<0.1			0.0611	0.03
H/C molar ratio		1.436		1.92		1.41
O/C molar ratio		0.39		0.61		0.24
HHV (MJ kg ⁻¹)	36.06	24.9	36.06	21.41	19.8	31.44
LHV (MJ kg ⁻¹)					18.4	
TAN KOH (mg kg ⁻¹)		110		76		102.9
pH				3		3.6

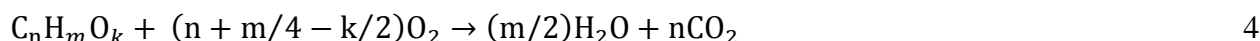
The quality of bio-oil obtained depends on the type of biomass used and the severity of process parameters such as temperature, gas residence time and heating rate [24]. Bio-oil can be directly used as fuel in boilers or gas turbines or subsequently upgraded to produce automobile fuels and bulk chemicals using several methods such as zeolite catalytic cracking, hydrogenation, and aqueous phase processing [25].

Synthesis gas (syngas) can be produced from hydrocarbons by either reforming or partial oxidation. The most widely used process is the steam reforming of methane carried out in tubular

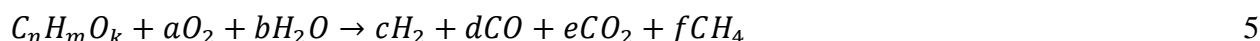
reactors. Steam reforming (SR) is an endothermic process causing it to be very energy intensive. Reformers are designed to optimize heat exchange and recovery leading to huge capital investments [26-28]. The SR of methane for example, is carried out at pressures of 1.4–4.0 MPa and temperatures ranging between 750–900 °C [29]. A number of thermodynamic and experimental studies have been performed on the SR of oxygenated organic compounds (oxygenates) in general and bio-oil in particular [5,30-34]. The general equation for the SR of oxygenates is given by reaction 1. This is an endothermic reaction and the amount of heat required depends on the value of the coefficients n, m and k . More hydrogen is produced subsequently via the water gas shift (WGS) reaction as CO reacts with water (reaction 2).



It is noteworthy that, given its mild exothermicity, the WGS reaction is favoured at temperatures well below those used for SR and so, if a single reactor is to be used under isothermal conditions, an optimum temperature has to be selected for which both reactions combine to give maximum hydrogen yield. Otherwise, maximum yields are obtained using separate reactors operated at high and low temperatures respectively [35,36]. Partial oxidation (POX) involves the use of sub-stoichiometric combustion oxygen to produce synthesis gas from hydrocarbons. It can be operated either thermally or catalytically but the overall hydrogen yield is lower than that obtained for SR due to the absence of steam as an extra source of hydrogen and because some hydrogen oxidizes to form water [37]. POX is exothermic and can appear to produce syngas at a lower cost since SR requires energy to sustain the endothermic SR reaction and generate steam [38]. The POX of oxygenates is given in reaction 3. The amount of energy released by this reaction depends on the particular oxygenated feedstock. The amount of oxygen used is very critical during POX as the use of stoichiometric oxygen will lead to complete oxidation (COX–reaction 4).



Autothermal reforming (ATR) is a process that uses steam and oxygen to produce synthesis gas. ATR reactors are designed to couple endothermic SR with exothermic POX so as to obtain a thermoneutral (adiabatic) or slightly exothermic process [39-41]. This coupling helps to reduce the overall cost of the synthesis gas produced compared to SR and also achieves a higher hydrogen yield compared to pure POX process [42,43]. ATR systems in which both partial oxidation and steam reforming reactions occur in a single catalytic bed are mostly useful for fuel cell applications. Those which have a separate burner for complete oxidation (combustion zone) followed by a catalytic bed for steam reforming are ideal for gas to liquid applications [44]. The overall reaction occurring during the ATR of bio-oil (or any oxygenated fuel) can be written as shown in reaction 5 [45].



The stoichiometric coefficients $c, d, e,$ and f depend on the amount of oxygen and steam (a and b) and also on temperature and extent of side reactions [31]. Some important side reactions which may occur together with SR, POX, WGS and COX include:

Decomposition:



Methanation of carbon:



Boudouard reaction:



Gasification:



Methane dry reforming:



Unlike methane and other fossil fuels, the use of bio-oils as feedstock to generate hydrogen (or synthesis gas) presents some tough challenges because of their very heterogeneous composition and thermal instability [10,31,46]. The main challenge is the formation of coke due to dehydration and polymerisation reactions which can be mitigated by using excess steam, bio-oil blending and appropriate catalyst choice [38,47]. Czernik and French [37] performed ATR of oak, poplar and pine bio-oils using 0.5% Pt/Al₂O₃ catalyst. They were able to produce 9–11 g of H₂ per 100 g of bio-oil (corresponding to 70 to 83% of stoichiometric potential) while varying temperature 800–850 °C, steam to carbon ratio 2.8–4.0 and oxygen to carbon ratio 0.9–1.1. Problems with volatility lead to the 11%–30% of bio-oil carbon forming deposits in the evaporator.

In order to optimise the ATR of bio-oil, it is important that the contributions of participating reactions in determining equilibrium product concentrations are known, bearing in mind the additional complexity stemming from using bio-oil as a feedstock. To the authors' knowledge, no work has been published on this aspect of bio-oil ATR reforming and this work is an attempt to contribute to this knowledge gap.

2. Materials and Method

2.1. Bio-oil composition generation

Due to the enormous variability in chemical composition that exists among bio-oils produced from different biomass sources [48], most thermodynamic equilibrium simulations have been carried out with the use of model compounds to simulate bio-oil feedstock in SR, POX, and ATR studies. Among these model compounds, acetic acid has received the most attention [49–51]. Other compounds such as cresol, acetone and ethylene glycol have also been used [31,47,52]. Even when the same biomass feedstock is used, variations in process parameters lead to different bio-oil compositions. Sukiran et al. [21] studied the effects of pyrolysis temperatures, particle sizes and heating rates on the yield of bio-oil from PEFB. They found significant differences in the bio-oil obtained when these process parameters were varied in the following ranges: temperature 300–700 °C, heating rate 10–100 °C min⁻¹, particle size <90, 91–106, 107–125 and 126–250 μm.

Using information from existing literature, the moisture free (mf) elemental compositions of some PEFB bio-oils were determined. The results are summarized in Table 2. Mean elemental compositions were determined excluding the results from [22] due to the low H/C ratio and high O/C ratio reported.

Table 2. Moisture free (mf) PEFB bio-oil elemental composition (mole fractions).

Author	C	H	O	N	H/C	O/C
[22]	0.4099	0.4137	0.1730	0.0001	1.0092	0.4220
[21]	0.3575	0.5032	0.1274	0.0119	1.4076	0.3565
[16]	0.3506	0.5001	0.1353	0.0140	1.4262	0.3858
[18]	0.3780	0.5654	0.0531	0.0035	1.4955	0.1406
[23]	0.3983	0.5173	0.0743	0.0101	1.2988	0.1865
[15]	0.3774	0.5659	0.0531	0.0035	1.4995	0.1407
Mean Elemental composition	0.3724	0.5304	0.0886		1.4243	0.2381

The mean over five mf elemental compositions obtained for PEFB bio-oil was $C_{0.3724}H_{0.5304}O_{0.0886}$ for which the nitrogen content was neglected. Acetic acid, phenol, levoglucosan, palmitic acid and furfural were selected as representative compounds found in PEFB bio-oil, since their presence in PEFB bio-oil has been repeatedly detected in significant amounts via GC-MS semi-quantitative analyses [9,53,54]. Other authors have performed thermodynamic analysis of complex mixtures by using mixtures of simpler compounds with the same molar elemental compositions. Zin et al. [55] used mixtures of acetic acid, levoglucosan, vanillin and furanone to perform the thermodynamic analysis of pine bio-oil aqueous fraction steam reforming. Hanika et al. [56] used a mixture of glucose, vanillin, n-butyl-stearate, methionine and tri-ethyl-phosphate as representative compounds to simulate the partial oxidation of rape meal. Table 3 gives the physical properties of acetic acid, phenol, levoglucosan, palmitic acid and furfural.

Table 3. Physical properties of model compounds found in PEFB bio-oil.

Properties	Acetic acid	Phenol	Levoglucosan	Palmitic acid	Furfural
Molecular formula	$C_2H_4O_2$	C_6H_6O	$C_6H_{10}O_5$	$C_{16}H_{32}O_2$	$C_5H_4O_2$
Heat of formation (gas) (kJ/mol)	-433	-95		-730	-149.6
Heat of combustion (liquid) (kJ/mol)	-874	-3058 (solid)	-2832 (solid)	-9977	-2339
Melting point (K)	289	314	455	336	237
Boiling point (K)	391	455	657	624	435
Flash point (K)	313	352	459	386	335
Density (g cm ⁻³)	1.043	1.0545@45 °C	1.688	0.8527@62 °C	1.155

Using the Solver function in Microsoft[®] Office Excel 2013 (MS Excel), it was possible to generate five PEFB bio-oil surrogates with similar elemental composition by considering different mixtures of the five representative compounds mentioned above. The Solver function has been demonstrated by other authors to be a very versatile and useful tool in performing chemical

engineering calculation [57,58]. The bio-oil surrogates were numbered BOS1-5. The relative error on the elemental composition for the different surrogates was less than 2% when compared to the mean elemental composition (see Table 4).

Table 4. Model PEFB bio-oils obtained using different combinations of acetic acid, phenol, levoglucosan, palmitic acid and furfural. Target composition: $C_{0.3724}H_{0.5304}O_{0.0886}$.

	BOS1	BOS2	BOS3	BOS4	BOS5
Name	mol (%)				
Acetic acid	12.2	23.2	0.0	0.3	0.0
Phenol	35.1	45.2	36.0	65.3	12.2
Levoglucosan	2.2	0.3	8.6	16.4	0.0
Palmitic acid	20.0	16.3	21.6	17.5	25.5
Furfural	30.5	15.0	33.8	0.5	62.2
TOTAL	100.0	100.0	100.0	100.0	100.0
C	0.3724	0.3724	0.3724	0.3724	0.3740
H	0.5390*	0.5390*	0.5372	0.5390*	0.5374*
O	0.0886	0.0886	0.0904*	0.0886	0.0886
Maximum relative error* (%)	1.6	1.6	2	1.3	1.3

* For a given surrogate, only the maximum elemental relative error, when compared to the average value, is shown. For BOS1, 2, 4 and 5, error shown for H, for BOS3, error shown for O.

2.2. Solution method of CEA

Chemical Equilibrium with Applications (CEA) software developed by National Aeronautics and Space Administration (NASA) was used to perform thermodynamic equilibrium simulations. The software determines the equilibrium properties of a reaction mixture by using the Gibbs free-energy-minimisation method based on a known pool of reactant and species, and user defined initial composition, temperature and pressure [59]. This method takes into consideration the fact that the total Gibbs free energy of a reacting system reaches a minimum at equilibrium when varying the mixture composition at constant pressure and temperature.

For a given mixture with a number K of species, the Gibbs free energy can be written as:

$$G = \sum_{i=1}^K \mu_i n_i \quad 6$$

where G is the Gibbs free energy, μ_i is the chemical potential of species i and n_i the number of moles of species i . The condition of equilibrium is the minimisation of G . In order to find the n_i that minimize the value of G , it is necessary that the values of n_i satisfy certain constraints, one of which is the elemental mass balance given by

$$\sum_{i=1}^K a_{ji} n_i - b_j^0 = 0 \quad 7$$

or

$$b_j - b_j^0 = 0 \quad (j=1, \dots, M) \quad 8$$

where a_{ji} are the number of gram atoms of element j per gram mole of species i and b_j^0 is the number of gram atoms of element j in the reaction mixture.

Using Lagrangian multipliers, G can be written as

$$G = g + \sum_{j=1}^M \lambda_j (b_j - b_j^0) \quad 9$$

where λ_i are Lagrangian multipliers and g the Gibbs free energy per gram of reaction mixture. Based on these equations, the condition for equilibrium can be expressed as:

$$G = \sum_{i=1}^K n_i \Delta G_i^0 + RT \sum_{i=1}^K n_i \ln y_i + RT \sum_{i=1}^K n_i \ln P \quad 10$$

where ΔG_i^0 is the standard Gibbs free energy of formation of species i , R is the universal gas constant, T is the temperature in Kelvin, y_i is the mole fraction of species i , and P is the total pressure.

The thermodynamic state for which the equilibrium composition is determined has to be specified by two intensive properties which, in principle, can be any combination of: temperature (T), pressure (P), specific enthalpy (h), specific entropy (s) and specific volume (v). In CEA, the “tp” setting is used for constant temperature and pressure processes, and the “hp” setting is used for constant pressure and enthalpy (adiabatic) processes. To solve equation 10, an iteration procedure is used with the Newton-Raphson method applied to solve for corrections to the initial estimates for composition, n_i , Lagrangian multipliers, moles of gaseous species and (when required) temperature, T [59].

All inputs into the CEA software were based on a bio-oil feedstock carbon number of 1500 (user-chosen arbitrarily). This carbon number was also used to calculate the amount of water and oxygen needed for ATR based on the desired steam to carbon ratio (S/C) and amount of oxygen expressed as the equivalence ratio, Φ , as used to describe oxy-combustion processes (actual O_2 to fuel molar ratio divided by stoichiometric combustion O_2 to fuel molar ratio). All temperatures were entered in Kelvin (K) and pressures in atmosphere (atm).

Thermodynamic simulation executed in CEA generates an output file containing all relevant thermodynamic properties and an equilibrium composition in mole fractions. To obtain the molar yields of equilibrium products, the mole fractions were converted to moles using a carbon balance. The total number of moles at equilibrium was determined using equation 11.

$$\text{total moles} = \frac{n_c}{\sum_{i=1}^j c_i x_i} \quad 11$$

where n_c is the initial (input) moles of carbon in the feed which in this case is equal to the chosen carbon number of 1500, j is the number of carbon containing species at equilibrium, and c_i and x_i are the carbon number and mole fraction respectively of the species i considered. Once the total moles of equilibrium species was determined, the equilibrium yields n_i of each species present were calculated using equation 12.

$$n_i = x_i \times \text{total moles} \quad 12$$

For each set of process condition considered, the overall performance was evaluated using critical factors such as hydrogen yield (Y_{H_2} , in wt% of the mf feed), and the percentage selectivity (X_i) to CH_4 , CO and CO_2 (see equations 13–16).

$$Y_{H_2} = \frac{\text{mass of } H_2 \text{ at equilibrium}}{\text{initial mass of bio-oil}} \times 100 \quad 13$$

$$X_{CH_4} = \frac{\text{moles of } CH_4}{\text{total moles of all carbon products}} \times 100 \quad 14$$

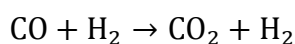
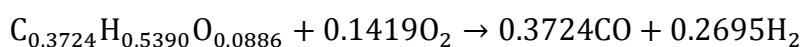
$$X_{CO} = \frac{\text{moles of } CO}{\text{total moles of all carbon products}} \times 100 \quad 15$$

$$X_{CO_2} = \frac{\text{moles of } CO_2}{\text{total moles of all carbon products}} \times 100 \quad 16$$

2.3. Modelling the global reactions of bio-oil ATR

It has been established in existing literature that several reactions are involved when biofuels (or organic fuels in general) undergo reforming to produce H_2 or syngas [10,60-62]. In order to eventually optimise the ATR of bio-oil, it is helpful to devise a tool that can be used to predict the contribution of the different participating reactions. The CEA software determines equilibrium composition by applying numerical techniques which are independent of the actual reaction mechanisms taking place. To determine possible reaction mechanisms, different sets of reactions were proposed and then tested to see how well they could fit the equilibrium yields obtained using CEA. Mechanism testing was performed algebraically using the Solver function in MS Excel. A mechanism was accepted as correct if predicted equilibrium concentrations with the proposed mechanism were close to actual equilibrium concentrations for all species with a relative percent error less than or equal to 1%.

As an example, suppose we propose a mechanism for ATR of bio-oil for which only three reactions, POX, SR, and WGS are assumed to occur. The following equations can be written for BOS1:



Let the moles of BOS1 (n_{BOS1}) consumed by POX and SR reactions be n_{POX} and n_{SR} respectively; and n_{WGS} the moles of carbon monoxide (CO) consumed by the WGS reaction. The general material balance equation for a particular species can be written as:

$$\text{Input} + \text{Generation} - \text{Consumption} = \text{Output} + \text{Accumulation} \quad 17$$

Given that the calculations are performed for a system at equilibrium there is no accumulation term and the other terms will depend on the particular chemical species considered. Applying equation 17 to our example, we can write the following equations to predict equilibrium concentration (in moles) of the chemical compounds involved:

$$n_{CO} = 0.3724n_{POX} + 0.3724n_{SR} - n_{WGS} \quad 18$$

$$n_{CO_2} = n_{WGS} \quad 19$$

$$n_{H_2} = 0.2695n_{POX} + 0.5533n_{SR} + n_{WGS} \quad 20$$

$$n_{BOS1} = n_{POX} + n_{SR} \quad 21$$

The number of predicted chemical species has to be equal to the number of equations in order for system to produce a unique solution. This system consisting of 4 equations and 4 unknowns is entered in Excel such that

$$\begin{pmatrix} 0.3724 & 0.3724 & -1 \\ 0 & 0 & 1 \\ 0.2695 & 0.5533 & 1 \\ 1 & 1 & 0 \end{pmatrix} \begin{pmatrix} n_{POX} \\ n_{SR} \\ n_{WGS} \end{pmatrix} = \begin{pmatrix} n_{CO} \\ n_{CO_2} \\ n_{H_2} \\ n_{BOS1} \end{pmatrix}$$

By substituting random values for n_{POX} , n_{SR} , and n_{WGS} it is possible to generate estimated equilibrium yields of CO, CO₂ and H₂ corresponding to an input moles of bio-oil (i.e. n_{CO} , n_{CO_2} , n_{H_2} and n_{BOS1}). These calculated values are then compared to the actual (desired) equilibrium concentration values and an error between both sets of values calculated. A solution is accepted if the errors for each species are below 1%, and the combined sum of errors is also below 5%.

Using the ATR equilibrium data generated by the CEA software, different combinations of reactions shown in Table 5 where tested using the methodology described above. Any number of the reactions given in Table 5 can occur during ATR of bio-oil. An acceptable mechanism should be able to account for all chemical species present at equilibrium and must contain equations which account for the following processes: bio-oil degradation, oxygen consumption, steam consumption, carbon formation, methane formation, carbon removal and methane removal.

Table 5. List of all reactions considered during bio-oil ATR mechanism modelling.

Name	Abbreviation	Reaction
1 Partial oxidation	POX	$C_nH_mO_k + (n-k)/2O_2 \rightarrow nCO + m/2H_2$
2 Complete oxidation	COX	$C_nH_mO_k + (n+m/4-k/2)O_2 \rightarrow nCO_2 + m/2H_2O$
3 Steam reforming	SR	$C_nH_mO_k + (n-k)H_2O \rightarrow nCO + (2n+m-2k)/2H_2$
4 Decomposition	DEC	$C_nH_mO_k \rightarrow kCO + m/2H_2 + (n-k)C$
5 Water gas shift*	WGS	$CO + H_2O \leftrightarrow CO_2 + H_2$
6 Boudouard reaction	BO-RX	$2CO \rightarrow CO_2 + C$
7 Methanation of C _(s)	MEN	$C_{(s)} + 2H_2 \rightarrow CH_4$
8 Carbon gasification 1	C-GS1	$C_{(s)} + H_2O \rightarrow CO + H_2$
9 Carbon gasification 2	C-GS2	$C_{(s)} + 0.5O_2 \rightarrow CO$
10 Methane steam reforming	ME-SR	$CH_4 + H_2O \rightarrow CO + 3H_2$
11 Carbon monoxide oxidation	CO-OX	$CO + 0.5O_2 \rightarrow CO_2$
12 Hydrogen oxidation	H-OX	$H_2 + 0.5O_2 \rightarrow H_2O$

* The reverse of the water gas shift reaction (R-WGS) was used in some cases

3. Results and Discussions

3.1. Sensitivity analysis and product distribution

The influence of bio-oil chemical composition on hydrogen yield was investigated. ATR was performed on the five bio-oil surrogates considered in this study by varying S/C ratio and amount of oxygen. The amount of oxygen used during ATR was expressed in terms of the equivalence ratio, Φ , which in this case was defined as the ratio of actual moles of oxygen/moles of carbon present in the reaction mixture to the stoichiometric moles of oxygen/moles of carbon needed for complete oxidation (COX) of the bio-oil feedstock. This is written mathematically as

$$\Phi = \frac{\text{Actual moles of } O_2/\text{moles of carbon in bio-oil}}{\text{Stoichiometric moles of } O_2\text{ needed for COX}/\text{moles of carbon in bio-oil}} \quad 22$$

The equivalence ratio was preferred over the more traditional O_2/C ratio because it highlights the relative amount of oxygen in the system and indicates how far off the system is from complete oxidation (combustion). By dividing the moles of oxygen needed for the stoichiometric partial oxidation of the bio-oil with that needed for its stoichiometric complete oxidation (see reaction 3 and 4) we can define the special value of equivalence ratio for stoichiometric partial oxidation, Φ_{POX} (equation 23).

$$\Phi_{POX} = \frac{\text{Stoichiometric moles of } O_2\text{ needed for POX}/\text{moles of carbon in bio-oil}}{\text{Stoichiometric moles of } O_2\text{ needed for COX}/\text{moles of carbon in bio-oil}} = \frac{\frac{n-k}{2}}{n + \frac{m-k}{4} \frac{k}{2}} \quad 23$$

Φ_{POX} was equal to 0.31 for all five bio-oil surrogates. Other equivalence ratios used in this study were obtained by considering 50%, 150%, and 200% of this value. Therefore for a given S/C ratio, the equivalence ratio considered were $\Phi = 0.15, 0.31 (\Phi_{POX}), 46,$ and 0.61 (corresponding to molar O_2/C of 0.19, 0.38, 0.57, and 0.76).

For all five bio-oil surrogates, equilibrium hydrogen yield and product concentrations were similar for all ATR equilibrium conditions examined. The maximum standard error obtained when comparing mean hydrogen yields from all five bio-oil surrogates was 0.324, corresponding to a percent error of 3.1%. This was obtained for S/C ratio = 4 and $\Phi = 0.15$ (Figure 1). This implies that equilibrium product distribution is insensitive to exact bio-oil composition. The minimal variations in mean hydrogen yield observed were due to the slight difference in elemental composition among the bio-oil surrogate mixtures.

The bio-oil surrogate mixtures all undergo similar reactions when subjected to the same oxidizing conditions. Zin et al. [55] also found that chemical equilibrium products from the SR of different mixtures of simulated aqueous fraction of pine bio-oil were the same. Table 6 shows mean equilibrium temperatures and their standard deviations obtained during the ATR of the five bio-oil surrogate mixtures. The equilibrium temperatures are almost equal for similar conditions of steam and oxygen with the maximum percent error of 1.6% obtained for S/C = 1 and $\Phi = 0.30$. This provided further evidence that ATR proceeds with a similar mechanism for all bio-oil surrogates and the equilibrium product composition depends on the final equilibrium (exit) temperature.

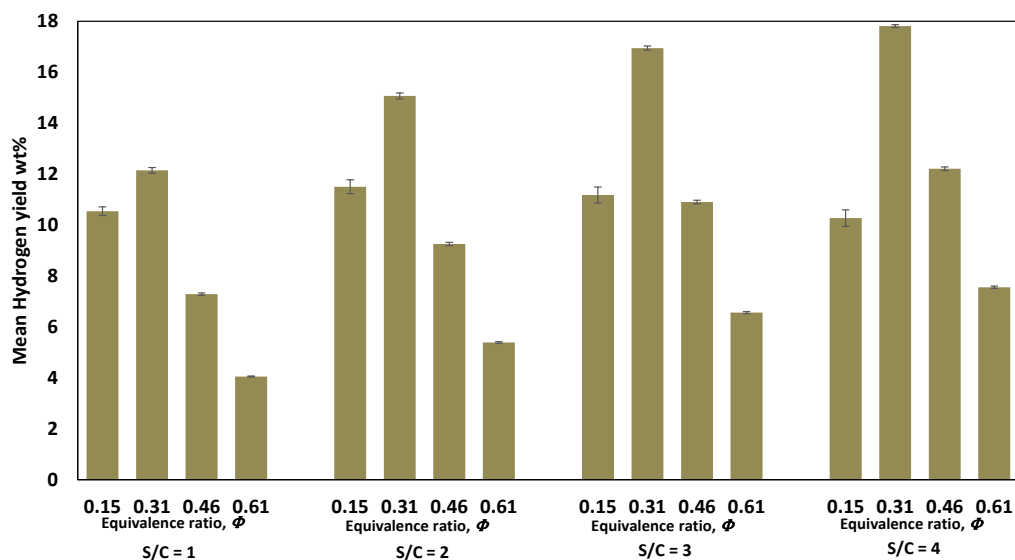


Figure 1. Mean hydrogen yield (BOS1-5) and standard error for Φ (0.15–0.61) and S/C (1–4).

Table 6. Mean temperatures (K) and standard deviations obtained during ATR of the five bio-oil surrogates (BOS1-5) considered in this study.

Equivalence ratio, Φ	S/C = 1	S/C = 2	S/C = 3	S/C = 4
$\Phi_1 \approx 0.15$	874 ± 4	804 ± 4	755 ± 4	715 ± 4
$\Phi_2 \approx 0.31$	1204 ± 19	1043 ± 13	942 ± 10	871 ± 7
$\Phi_3 \approx 0.46$	1963 ± 19	1587 ± 14	1370 ± 11	1225 ± 9
$\Phi_4 \approx 0.61$	2521 ± 12	2079 ± 13	1773 ± 11	1566 ± 9

At constant S/C ratio, increasing the amount of oxygen (equivalence ratio) causes the exothermic oxidation reaction to become more favourable leading to an overall increase in the temperature of the system. On the other hand, increasing S/C ratio at constant Φ reduces the equilibrium temperature due to the high heat capacity of water which absorbs some of the surrounding heat without causing a temperature increase.

Figure 2a shows the influence of the S/C ratio on the equilibrium hydrogen yield for the ATR of BOS2. BOS2 was used to discuss all remaining results because its composition is more realistic when compared to that of bio-oils found in published literature. As expected, the amount of equilibrium hydrogen increased with increase in S/C ratio. The maximum hydrogen yield obtained was about 12 wt% at S/C = 1 and increased to about 18wt% at S/C = 4. This was due primarily to increase in water gas shift reaction which shifts to the right (towards forming more products) as more steam is introduced in the system.

For all S/C ratios, the maximum hydrogen yield was obtained at values of Φ close to Φ_{POX} (0.31) that is, when the amount of oxygen in the system was close to that needed for stoichiometric partial oxidation. A closer look (Figure 2b) reveals that at low S/C ratios (1 and 2), the maximum hydrogen yields occurred at equivalence ratio lower than Φ_{POX} ($\Phi \approx 0.27$) but attained this value at S/C = 4. Φ_{POX} is therefore an important parameter that can be used to determine the amount of oxygen to use during ATR in order to achieve maximum hydrogen yield.

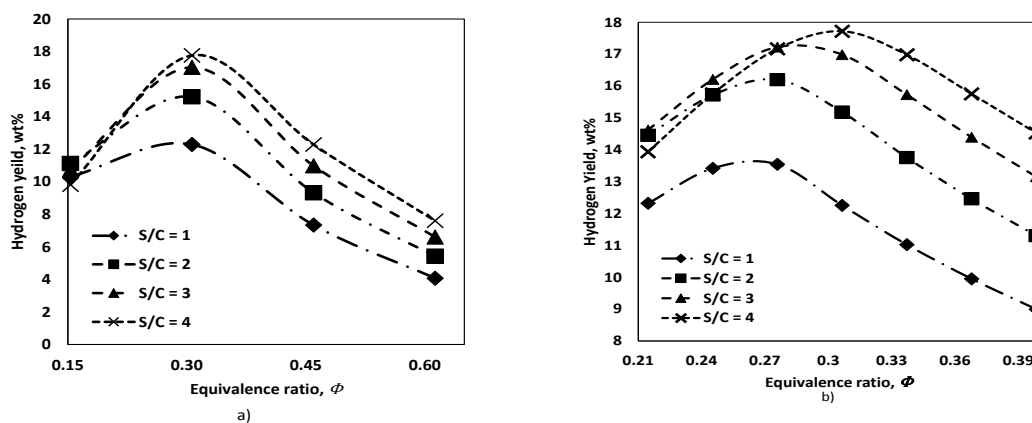


Figure 2. Influence of S/C ratio and the equivalence ratio on the amount of hydrogen produced during the ATR of BOS2. (a) ϕ range 0.15–0.61, (b) refined ϕ scale (0.21–0.39).

3.2. Selectivity to carbon containing products

The influence of S/C ratio and amount of oxygen on the selectivity to carbon containing products is shown in Figure 3. Overall, as more steam is added, the product gas becomes increasingly rich in CO_2 . In Figure 3a, solid carbon (in the form of graphite), CH_4 , CO_2 and CO are all present at the lowest equivalence ratio considered in this study. The presence of carbon and methane is an indication of possible bio-oil thermal decomposition and Boudouard reaction. Both reactions are known to occur under oxidant deficient conditions [47]. As more oxygen is added, carbon and CH_4 essentially become negligible and CO remains as the major product.

The decrease in carbon and CH_4 concentrations observed between $\phi = 0.15$ and 0.30 (Figure 3a) is due to carbon gasification and methane steam reforming respectively (reaction 8 and 10 on Table 5). Both reactions directly contribute in increasing the H_2 concentration and CO selectivity. The high CO content indicates that virtually no water gas shift reaction takes place under this process condition. The decrease in CO_2 concentration that occurs between $\phi = 0.3$ and 0.45 is due to the reverse water gas shift reaction which become favorable at high temperatures (1204–1963 K). The slight increase in CO_2 observed $\phi > 0.45$ is due to the bio-oil undergoing combustion (complete oxidation) producing CO_2 and H_2O . The same trends as just explained hold for Figure 3b–d. The main difference being that as the S/C ratio is increased to 2, 3, and 4 respectively, the water gas shift reaction becomes increasingly prominent, converting most of the CO in the system to CO_2 .

3.3. Synthesis gas composition

Hydrogen or synthesis gas can be used as a primary feedstock in fuel cells or as feed for downstream chemical synthesis. Depending on the end use of the synthesis gas produced, the ATR process can be operated by choosing appropriate values for S/C ratio and amount of oxygen (ϕ) to give a desired synthesis gas composition [63].

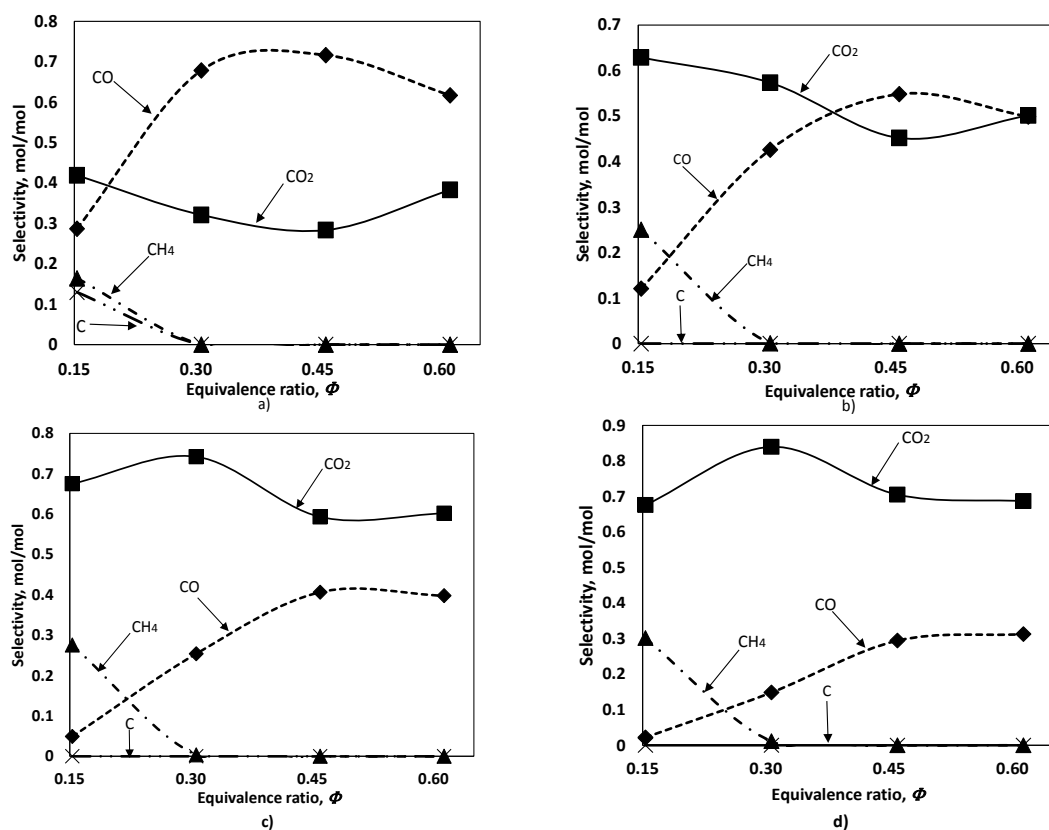


Figure 3. Influence of S/C ratio and O₂/C ratio on the selectivity of carbon and carbon containing products during the ATR of BOS2 at 1 atm. a) S/C = 1 b) S/C = 2 c) S/C = 3 d) S/C = 4.

3.3.1. Fuel cell feed

Fuel cells are electrochemical devices which convert the chemical energy of a chemical reaction directly into electrical and thermal energy [64]. Generally speaking, there are five types of hydrogen fuel cells divided into two main categories: low-temperature fuel cells and high-temperature fuel cells. The low-temperature fuel cells such as polymer electrolyte membrane fuel cell (PEMFC), alkaline fuel cell (AFC), and phosphoric acid fuel cell (PAFC) operate at temperatures ranging between 370–473 K and use hydrogen as their only fuel source with very little tolerance for CO (<20 ppm for PEMFC) [43,65]. For such fuel cells, the output gas from an autothermal reformer will have to be purified and all CO₂, CO and unreacted feedstock removed to give an essentially pure hydrogen stream. To reduce the cost of the downstream purification, the ATR process will have to be operated under conditions of maximum hydrogen yield for a given S/C ratio and amount of oxygen (see Figure 2). Purification can then be achieved by using CO₂ absorbent, pressure swing adsorption systems and catalytic preferential oxidation [43,66].

The high-temperature fuel cells include molten carbonate fuel cell (MCFC) and sulphur oxide fuel cell (SOFC). These fuel cells operate at much higher temperatures ranging between 923–1273 K and show more flexibility in feedstock and catalyst requirements [64]. For these fuel cells, hydrogen competes with CO and even CH₄ as fuel source making the combined H₂+CO from ATR an important parameter. Figure 4 shows the influence of ϕ and S/C ratio on total H₂+CO yield.

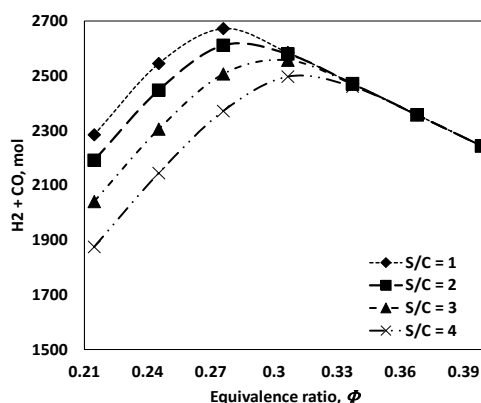


Figure 4. Influence of S/C ratio and Φ (amount of oxygen) on the total $H_2 + CO$ obtained during ATR of BOS2 at 1 atm.

The maximum total H_2+CO reduces as the S/C ratio is increased from 1 to 4. This happens because the formation of CH_4 becomes favorable at high S/C ratios and $\Phi < \Phi_{POX}$ (Figure 3). In the absence of methanation, the total H_2+CO remains the same ($\Phi > 0.33$) due the equal mole to mole ratio between H_2 and CO as one mole of CO converted to CO_2 via the water gas shift reaction gives one mole of H_2 . Irrespective of the S/C ratio chosen, optimal yield for H_2+CO is obtained at equivalence ratio approximately equal to Φ_{POX} .

3.3.2. Chemical synthesis feed

Synthesis gas is an important intermediate in the production of several important chemicals such as methanol, dimethyl ether (DME), ammonia and liquid fuels (via gas-to-liquid ‘GTL’ processes). These processes rely either on direct combination of reactants or Fischer-Tropsch (FT) chemistry and have different requirements in the amounts of H_2 , CO and CO_2 in synthesis gas. A key parameter for such processes is the H_2/CO ratio whose variation for the ATR of PEFB is shown in Figure 5.

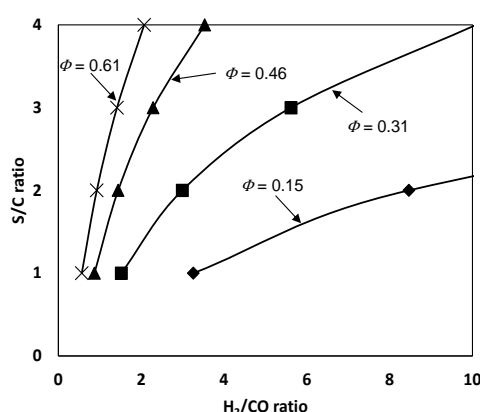


Figure 5. Plot of S/C ratio versus H_2/CO ratio at different values of Φ during ATR of BOS2. Equilibrium simulation carried out at 1 atm. The maximum H_2/CO ratio shown is 10.

Gas-to-liquid (GTL) Fischer-Tropsch processes for which only H₂ and CO are reactants require a H₂/CO ≈ 2 [36,67]. The synthesis gas in this case can be produced from an autothermal reformer operating with a S/C ratio between 1 and 2 and $\Phi < \Phi_{POX}$ (Figure 5). Synthesis of higher alcohols require H₂/CO = 1 [35]. In this case ATR can be performed at a low S/C ratio (S/C ≤ 1) and equivalence ratio slightly larger than the value required for stoichiometric partial oxidation, that is, $\Phi > \Phi_{POX}$ so as to avoid any carbon formation (Figure 3a). H₂, CO and CO₂ are all reactants in methanol, dimethyl ether and high temperature Fischer-Tropsch synthesis [68]. For such processes, the synthesis gas is made to have the same stoichiometry as the final product with its composition expressed as shown in equation 24.

$$M = \frac{H_2 - CO_2}{CO + CO_2} \quad 24$$

M is called the module and is equal to 2 for methanol and dimethyl ether synthesis [35,68]. For ATR, this value of M can only be obtained either by addition of H₂ or removal of CO₂. For BOS2 used in this study, the maximum value of M was 0.7 obtained at $\Phi = \Phi_{POX}$ for all S/C ratios examined. The explanations given in this section are simplified and meant to serve as a guide only. The eventual choice in process parameters will depend on other important factors like process scale and amount of product recycle [35,69].

3.4. Reaction mechanism

The advantage of using the Gibbs minimization energy is that a very large pool of chemical species is used to determine eventual equilibrium composition. The alternative will be to assume the prevailing reactions under the given process conditions and then use their equilibrium constants to determine equilibrium concentrations. The limitation of the latter is that fewer numbers of reactions and potential products are considered, compared to the number of species used by the Gibbs minimization method. Two main types of mechanisms were successful in accounting for equilibrium species obtained by the CEA software in the ATR of PEFB bio-oil. The results presented are those obtained from using BOS2 as feedstock. Similar results were obtained for all five bio-oil surrogates considered in this study. All reactions in this section are identified using the reaction nomenclature introduced in Table 5.

3.4.1. Partial oxidation (POX) based mechanism

The reactions considered for this mechanism were: bio-oil partial oxidation (POX), bio-oil steam reforming (SR), water gas shift (WGS), Boudouard reaction (BO-RX), methanation of carbon (MEN), carbon gasification (C-GS1 and C-GS2), methane steam reforming (ME-SR), hydrogen oxidation (H-OX) and carbon monoxide oxidation (CO-OX). These reactions were used to fit equilibrium results obtained at S/C = 1–4 and $\Phi = 0.31$ and 0.46. Not all reactions were involved at the same time for a given process condition. With a relative error less than 0.1% on individual molar production rates, it was impossible to distinguish between the mechanism-predicted and the equilibrium ('actual') values of H₂ yield as shown in Figure 6.

The contribution to hydrogen production by participating reactions for the POX based mechanism is shown in Figure 7. By way of this mechanism, hydrogen production was primarily

from POX, WGS and carbon gasification (C-GS1) at $\Phi = 0.31$ and by POX and SR at $\Phi = 0.46$. The implication of this mechanism is that under low oxygen content ($\Phi \leq \Phi_{POX}$), the bio-oil completely undergoes POX and that more hydrogen is produced by the water gas shift reaction with no significant contribution from SR. Further production of hydrogen is achieved by the gasification of all solid carbon formed. Meanwhile at the intermediate $\Phi = 0.46$ ($>\Phi_{POX}$), POX and SR were the only hydrogen producing reactions.

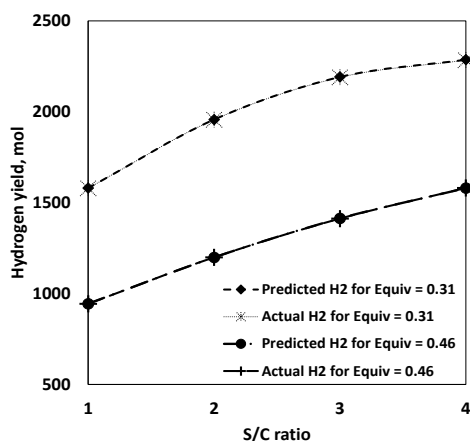


Figure 6. Comparing actual equilibrium hydrogen yield with predicted yield using POX based mechanism.

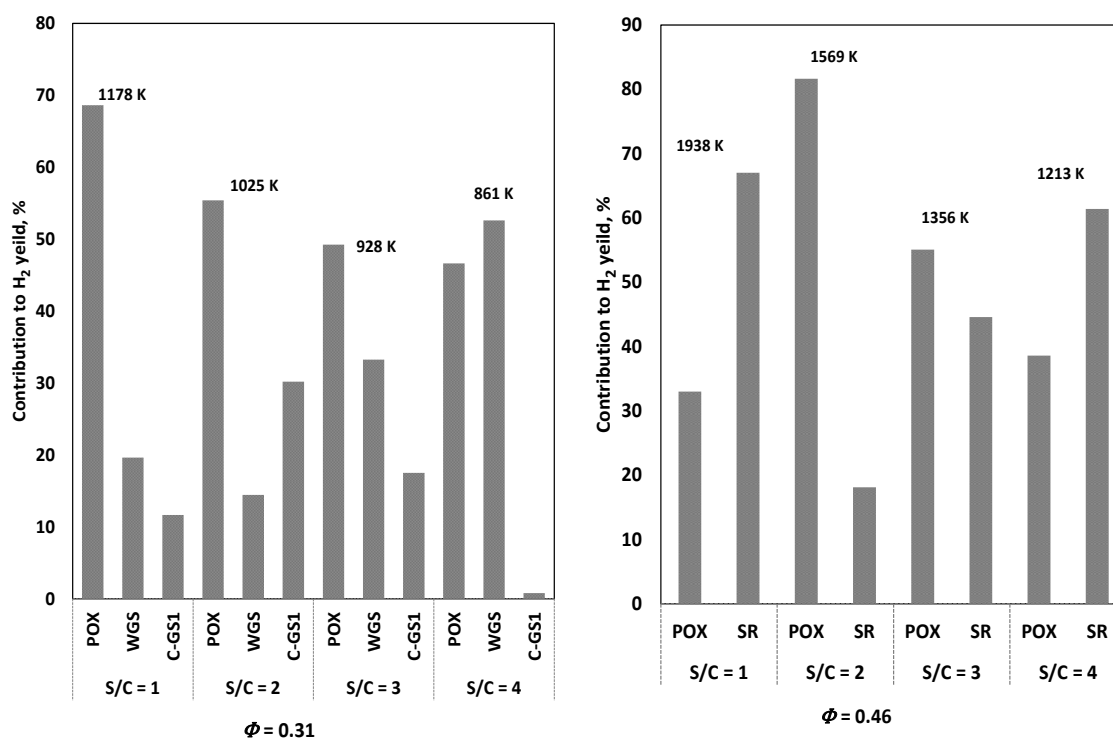


Figure 7. Percentage contribution to hydrogen production by participating reactions for the POX mechanism at (autothermal temperatures given in the figure for each S/C).

For this mechanism, no significant hydrogen consumption occurred as methanation of carbon (MEN) was virtually zero. In the case of $S/C = 1$ and $\Phi = 0.46$, H-OX and reverse WGS (R-WGS) were responsible for H_2 consumption. Figure 8 shows how the amount of steam and oxygen influenced the bio-oil consuming reactions.

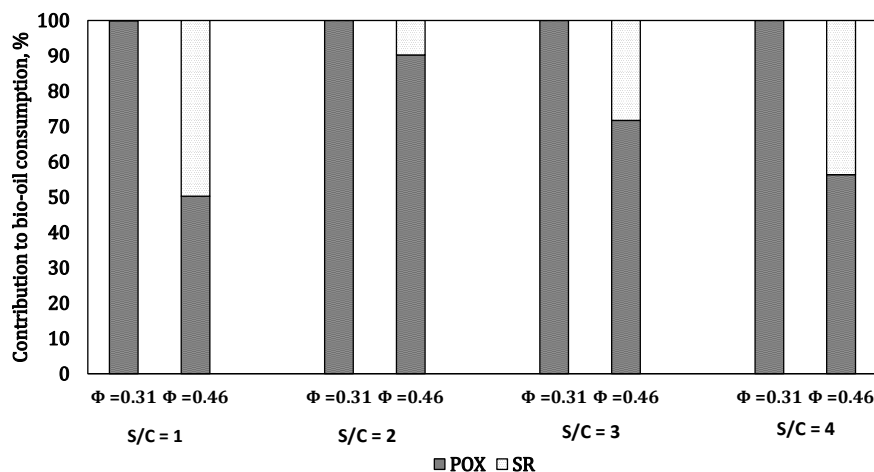


Figure 8. Influence of S/C ratio and oxygen on Bio-oil consuming reactions.

Table 7 gives a summary of the different reactions that dominate in the POX based mechanism at various temperature ranges. This table provides valuable information for the eventual choice of catalyst. For ATR carried out at temperature below 1100 K, the catalyst should be very selective to POX and WGS. High temperatures typical of low S/C ratios and high oxygen content ($\Phi \gg \Phi_{POX}$) should be avoided since they can lead to catalyst degradation.

Table 7. Summary of POX based mechanism based on temperature range. Only reactions which contribute to equilibrium products are included.

	$T < 1100 \text{ K}$	$1200 < T < 1600 \text{ K}$	$T > 1800 \text{ K}$
Steam content	$S/C > 2$	$2 < S/C < 4$	$S/C < 2$
Oxygen content	$\Phi < \Phi_{POX}$	$\Phi > \Phi_{POX}$	$\Phi \gg \Phi_{POX}$
Reaction condition	Catalytic	Catalytic and homogenous	Homogenous
Reactions	POX, WGS, BO-RX, MEN, C-GS1	POX, SR, C-GS2, CO-OX	POX, SR, R-WGS, H-OX, CO-OX

Based on this mechanism, it can be said that at $\Phi \leq \Phi_{POX}$, SR reactions are minimal and the choice of catalyst should be based on the prevailing POX, WGS and C-GS1 reactions.

3.4.2. Complete oxidation (COX) based mechanism

Another mechanism was validated for which complete oxidation (COX) was the dominant oxygen-consuming reaction. There was a near perfect agreement between the predicted hydrogen concentration and actual equilibrium hydrogen yield (Figure 9). The reactions considered for this mechanism were bio-oil thermal decomposition (DEC), bio-oil complete oxidation (COX), bio-oil

steam reforming (SR), WGS, reverse water gas shift (R-WGS), methane steam reforming (ME-SR), methanation of carbon (MEN), carbon gasification (C-GS1 and C-GS2), and hydrogen oxidation (H-OX), as shown in Figure 10.

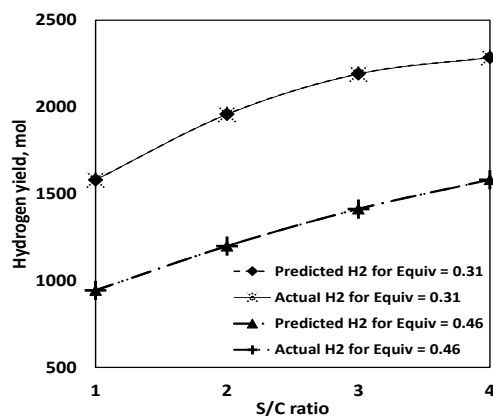


Figure 9. Plots of predicted hydrogen and actual equilibrium hydrogen showing near match with maximum relative error of 0.1% for the COX based mechanism.

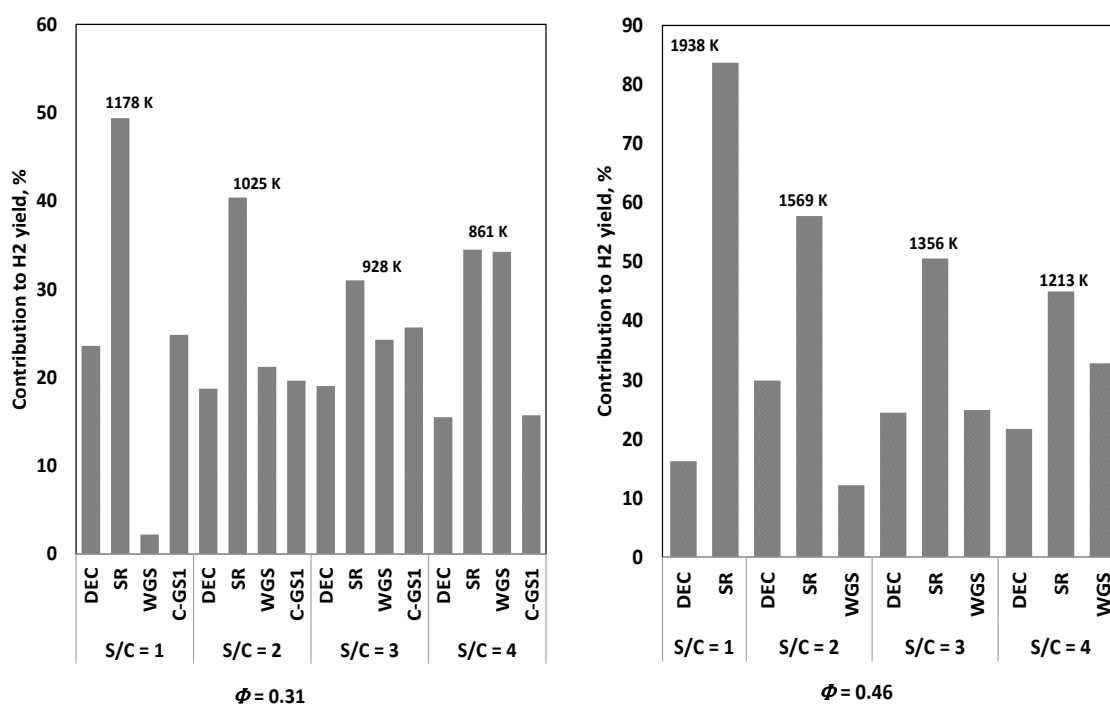


Figure 10. Percentage contribution to hydrogen production by participating reactions for the COX based mechanism (autothermal temperatures given in the figure for each S/C).

At $\phi = 0.31$, hydrogen production stemmed from DEC, SR, WGS and C-CG1. As expected more hydrogen was produced from WGS as the S/C ratio was increased from 1 to 4. A similar trend

was observed at $\Phi = 0.46$ except for the fact that there was no C-GS1 reaction. Carbon formed at the higher equivalence ratio is removed via reaction with oxygen (C-GS2).

For this mechanism, bio-oil was consumed almost in the same proportion among COX, SR and DEC independently of the amount of oxygen, as illustrated in Figure 11.

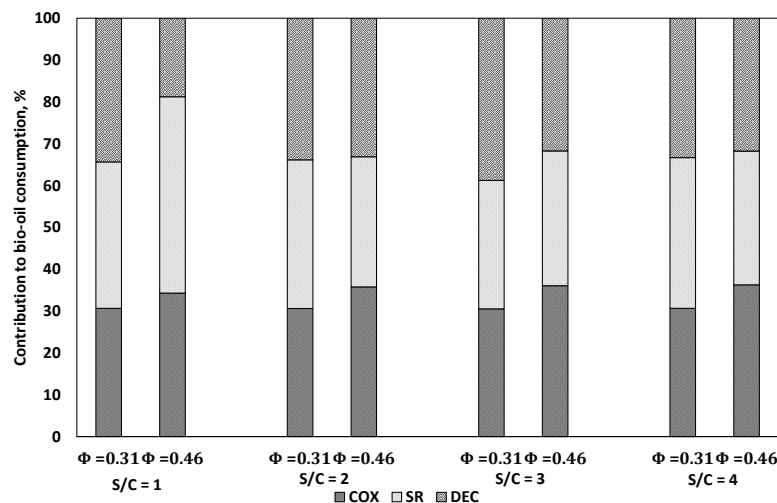


Figure 11. Influence of S/C ratio and oxygen on Bio-oil consuming reactions.

This mechanism relies on gas phase decomposition and combustion which occur significantly at all ATR conditions examined. Table 8 gives a summary of the different reactions that dominate in the COX based mechanism at various temperature ranges. A suitable catalyst for this mechanism will have to be very selective for COX, DEC, SR and C-GS1, as well as offering high thermal stability, although at high Φ , all reactions are expected to become homogeneous (non-catalytic) due to high autothermal temperatures.

Table 8. Summary of different COX mechanism based on temperature range. Only reactions which contribute to equilibrium products are included.

	T < 1100 K	1200 < T < 1600 K	T > 1800 K
Steam content	S/C > 2	2 < S/C < 3	S/C < 2
Oxygen content	$\Phi < \Phi_{POX}$	$\Phi > \Phi_{POX}$	$\Phi \gg \Phi_{POX}$
Reaction condition	Catalytic and homogenous	Catalytic and homogenous	Homogenous
Reactions	COX, DEC, SR, WGS, C-GS1,	COX, DEC, SR, C-GS1	COX, DEC, SR, R-WGS, C-GS2, H-OX

3.4.3. Comments on mechanisms

The POX and COX based mechanisms discussed above highlight the fact that there may be several routes leading to the formation of the desired H₂ and CO products autothermally. Such schemes are typical for systems where several reaction equilibria occur simultaneously [70]. For the

POX based mechanism to be realistic it has to be completely catalytic. An appropriate choice of catalyst can lead to the suppression of undesirable side reactions and products like carbon (coke). The COX based mechanism relies on homogenous oxidation and decomposition. Thermal decomposition accounts for about 30% of the bio-oil consumption and this can prove challenging to manage due to excessive carbon (coke) formation on reactor walls and catalyst and can be difficult to completely eliminate by gasification (depending on type of carbon formed). In addition, it might be necessary to operate under conditions of $\Phi > \Phi_{POX}$ in order to compensate for heat loss and feed preheating (sensible heat) [71].

4. Conclusion

This work demonstrates that ATR is, in theory, a viable process for the production of hydrogen-rich syngas from bio-oil. Using bio-oil surrogate mixtures with different compositions, it was established that hydrogen yield and concentration of other equilibrium products were insensitive to actual chemical composition. The molar elemental composition proved to be the determining factor for equilibrium hydrogen and syngas yield. The possibility of generating syngas with different H₂ and CO compositions by varying the S/C ratio and the equivalence ratio makes ATR of bio-oil a feasible option for applications like fuel cells and chemical synthesis. Mechanisms were proposed to account for equilibrium product yields. A POX based mechanism was proposed in which H₂ was produced from POX, SR and WGS. For this POX based mechanism, ATR can be viewed as partial oxidation combined with WGS instead of the more traditional notion of exothermic oxidation coupled with endothermic SR. Another mechanism validated was the COX based mechanism in which thermal decomposition accounted for about 30% of bio-oil consumption with hydrogen production assured by decomposition to carbon, steam reforming, water gas shift and carbon gasification reactions.

The equilibrium calculations performed in this study do not take into consideration the kinetic aspects of the reactions involved and could prove unrealistic in real ATR reactors [72]. The proposed mechanisms can only occur when equilibrium is attained for example working at low space velocities and high catalytic activity. Future work should therefore focus on kinetic studies and the influence of other process parameters like pressure and space velocity.

Conflict of interest

All authors declare no conflicts of interest in this paper.

References

1. Naik SN, Goud VV, Rout PK, et al. (2010) Production of first and second generation biofuels: A comprehensive review. *Renew sust energ rev* 14: 578-597.
2. Ni M, Leung DYC, Leung MKH, et al. (2006) An overview of hydrogen production from biomass. *Fuel process technol* 87: 461-472.
3. Ni M, Leung DYC, Leung MKH, et al. (2006) An overview of hydrogen production from biomass. *Fuel process technol* 87: 461-472.
4. Wu C, Huang Q, Sui M, et al. (2008) Hydrogen production via catalytic steam reforming of fast

- pyrolysis bio-oil in a two-stage fixed bed reactor system. *Fuel process technol* 89: 1306-1316.
5. Chattanathan SA, Adhikari S, Abdoulmoumine N (2012) A review on current status of hydrogen production from bio-oil. *Renew sust energ rev* 16: 2366-2372.
 6. Czernik S, Bridgwater AV (2004) Overview of Applications of Biomass Fast Pyrolysis Oil. *Energ fuel* 18: 590-598.
 7. Kamm B, Kamm M, Gruber PR, et al. (2005) Biorefinery Systems—An Overview. In: Kamm B, R GP, Kamm M, editors. *Biorefineries-Industrial Processes and Products: Status Quo and Future Directions*. Weinheim: Wiley-VCH Verlag GmbH, pp. 1-40.
 8. Jacobson K, Maheria KC, Dalai AK (2013) Bio-oil valorization: A review. *Renew sust energ rev* 23: 91-106.
 9. Mantilla SV, Gauthier-Maradei P, Gil PÁ, et al. (2014) Comparative study of bio-oil production from sugarcane bagasse and palm empty fruit bunch: Yield optimization and bio-oil characterization. *J anal appl pyrol* 108: 284-294.
 10. Czernik S, Evans R, French R (2007) Hydrogen from biomass-production by steam reforming of biomass pyrolysis oil. *Cataly today* 129: 265-268.
 11. Chang SH (2014) An overview of empty fruit bunch from oil palm as feedstock for bio-oil production. *Biomass bioenerg* 62: 174-181.
 12. Isahak WNRW, Hisham MWM, Yarmo MA, et al. (2012) A review on bio-oil production from biomass by using pyrolysis method. *Renew sust energ rev* 16: 5910-5923.
 13. Bridgwater AV (2012) Review of fast pyrolysis of biomass and product upgrading. *Biomass bioenerg* 38: 68-94.
 14. Abdullah N, Gerhauser H (2008) Bio-oil derived from empty fruit bunches. *Fuel* 87: 2606-2613.
 15. Sulaiman F, Abdullah N (2011) Optimum conditions for maximising pyrolysis liquids of oil palm empty fruit bunches. *Energy* 36: 2352-2359.
 16. Kim SW, Koo B, Ryu J, et al. (2013) Bio-oil from the pyrolysis of palm and Jatropha wastes in a fluidized bed. *Fuel process technol* 108: 118-124.
 17. Autaa M, Erna LM, Hameeda BH (2014) Fixed-bed catalytic and non-catalytic empty fruit bunch biomass pyrolysis. *J anal appl pyrol* 107: 67-72.
 18. Abdullah N, Gerhauser H, Sulaiman F (2010) Fast pyrolysis of empty fruit bunches. *Fuel* 89: 2166-2169.
 19. Akhtar J, Amin NAS (2011) A review on process conditions for optimum bio-oil yield in hydrothermal liquefaction of biomass. *Renew sust energ rev* 15: 1615-1624.
 20. Akhtar J, Kuang SK, Amin NS (2010) Liquefaction of empty palm fruit bunch (EPFB) in alkaline hot compressed water. *Renewable energy* 35: 1220-1227.
 21. Sukiran MA, Chin CM, Bakar N (2009) Bio-oils from Pyrolysis of Oil Palm Empty Fruit Bunches. *Am j appl sci* 6: 869-875.
 22. Pimenidou P, Dupont V (2012) Characterisation of palm empty fruit bunch (PEFB) and pinewood bio-oils and kinetics of their thermal degradation. *Bioresource technol* 109: 198-205.
 23. Khor KH, Lim KO, Zainal ZA (2009) Characterization of bio-oil: a by-product from slow pyrolysis of oil palm empty fruit bunches. *Am j appl sci* 6: 1647-1652.
 24. Ayabe S, Omoto H, Utaka T, et al. (2003) Catalytic autothermal reforming of methane and propane over supported metal catalysts. *Appl Catal a-gen* 241: 261-269.
 25. Rennard DC, Dauenhauer PJ, Tupy SA, et al. (2008) Autothermal Catalytic Partial Oxidation of Bio-Oil Functional Groups: Esters and Acids. *Energ fuel* 22: 1318-1327.

26. Dybkjaer I (1995) Tubular reforming and autothermal reforming of natural gas - an overview of available processes. *Fuel process technol* 42: 85-107.
27. Rabenstein G, Hacker V (2008) Hydrogen for fuel cells from ethanol by steam-reforming, partial-oxidation and combined auto-thermal reforming: A thermodynamic analysis. *J Power sources* 185: 1293-1304.
28. Rostrup-Nielsen T (2005) Manufacture of hydrogen. *Cataly today* 106: 293-296.
29. Jonga Md, Reindersa AHME, Kok JBW, et al. (2009) Optimizing a steam-methane reformer for hydrogen production. *Int j hydrogen energ* 34: 285-292.
30. Adhikari S, Fernando S, Gwaltney SR, et al. (2007) Athermodynamic analysis of hydrogen production by steam reforming of glycerol. *Int j hydrogen energ* 32: 2875-2880.
31. Vagia EC, Lemonidou AA (2008) Thermodynamic analysis of hydrogen production via autothermal steam reforming of selected components of aqueous bio-oil fraction. *Int j hydrogen energ* 33: 2489-2500.
32. Xie J, Su D, Yin X, et al. (2011) Thermodynamic analysis of aqueous phase reforming of three model compounds in bio-oil for hydrogen production. *Int j hydrogen energ* 36: 15561-15572.
33. Garcia L, French R, Czernik S, et al. (2000) Catalytic steam reforming of bio-oils for the production of hydrogen: effects of catalyst composition. *Appl catal a-gen* 201: 225-239.
34. Trane R, Dahl S, Skjøth-Rasmussen MS, et al. (2012) Catalytic steam reforming of bio-oil. *Int j hydrogen energ* 37: 6447-6472.
35. Rostrup-Nielsen JR, Sehested J, Nørskov JK (2002) Hydrogen and synthesis gas by steam- and CO₂ reforming. *Advance catalysis* 47: 65-139.
36. Aasberg-Petersen K, Dybkjær I, Ovesen CV, et al. (2011) Natural gas to synthesis gas – Catalysts and catalytic processes. *J nat gas sci eng* 3: 423-459.
37. Czernik S, French R (2014) Distributed production of hydrogen by auto-thermal reforming of fast pyrolysis bio-oil. *Int j hydrogen energ* 39: 744-750.
38. Rennard D, French R, Czernik S, et al. (2010) Production of synthesis gas by partial oxidation and steam reforming of biomass pyrolysis oils. *Int j hydrogen energ* 35: 4048-4059.
39. Kolios G, Frauhammer J, Eigenberger G (2000) Autothermal fixed-bed reactor concepts. *Chem eng sci* 55: 5945-5967.
40. Aasberg-Petersen K, Christensen TS, Stub Nielsen C, et al. (2003) Recent developments in autothermal reforming and pre-reforming for synthesis gas production in GTL applications. *Fuel Process technol* 83: 253-261.
41. Martin S, Wörner A (2011) On-board reforming of biodiesel and bioethanol for high temperature PEM fuel cells: Comparison of autothermal reforming and steam reforming. *J power sources* 196: 3163-3171.
42. Ruiz JAC, Passos FB, Bueno JMC, et al. (2008) Syngas production by autothermal reforming of methane on supported platinum catalysts. *Appl Catal a-gen* 334: 259-267.
43. Semelsberger T, Brown F, Borup RL, et al. (2004) Equilibrium products from autothermal processes for generating hydrogen-rich fuel-cell feeds. *Int j hydrogen energ* 29: 1047-1064.
44. Zahedi Nezhada M, Rowshanzamira S, Eikanic MH (2009) Autothermal reforming of methane to synthesis gas: Modeling and simulation. *Int j hydrogen energ* 34: 1292-1300.
45. Haynes DJ, Shekhawat D (2011) Chapter 6 Oxidative Steam Reforming. In: Shekhawat D, Spivey JJ, Berry DA, editors. *Fuel Cells: Technologies for Fuel Processing*. Amsterdam: Elsevier: 129-190.

46. Garcia La, French R, Czernik S, et al. (2000) Catalytic steam reforming of bio-oils for the production of hydrogen: effects of catalyst composition. *Appl catal a-gen* 201: 225-239.
47. Wu C, Liu R (2010) Carbon deposition behavior in steam reforming of bio-oil model compound for hydrogen production. *Int j hydrogen energ* 35: 7386-7398.
48. Hou T, Yuan L, Ye T, et al. (2009) Hydrogen production by low-temperature reforming of organic compounds in bio-oil over a CNT-promoting Ni catalyst. *Int j hydrogen energ* 34: 9095-9107.
49. Resende KA, Ávila-Neto CN, Rabelo-Neto RC, et al. (2015) Thermodynamic analysis and reaction routes of steam reforming of bio-oil aqueous fraction. *Renewable energy* 80: 166-176.
50. Wang S, Cai Q, Zhang F, et al. (2014) Hydrogen production via catalytic reforming of the bio-oil model compounds: Acetic acid, phenol and hydroxyacetone. *Int j hydrogen energ* 39: 18675-18687.
51. Latifi M, Berruti F, Briens C (2014) Non-catalytic and catalytic steam reforming of a bio-oil model compound in a novel “Jiggle Bed” Reactor. *Fuel* 129: 278-291.
52. García-García I, Acha E, Bizkarra K, et al. (2015) Hydrogen production by steam reforming of m-cresol, a bio-oil model compound, using catalysts supported on conventional and unconventional supports. *Int j hydrogen energ* 40: 14445–14455.
53. Zin RM, Lea-Langton A, Dupont V, et al. (2012) High hydrogen yield and purity from palm empty fruit bunch and pine pyrolysis oils. *Int j hydrogen energ* 37: 10627-10638.
54. Sembiring KC, Rinaldi N, Simanungkalit SP (2015) Bio-oil from Fast Pyrolysis of Empty Fruit Bunch at Various Temperature. *Energy procedia* 65: 162-169.
55. Zin RM, Ross AB, Jones JM, et al. (2015) Hydrogen from ethanol reforming with aqueous fraction of pine pyrolysis oil with and without chemical looping. *Bioresour technol* 176: 257-266.
56. Hanika J, Lederer J, Tukac V, et al. (2011) Hydrogen production via synthetic gas by biomass/oil partial oxidation. *Chem eng j* 176-177: 286-290.
57. Lima da Silva A, Malfatti CdF, Müller IL (2009) Thermodynamic analysis of ethanol steam reforming using Gibbs energy minimization method: A detailed study of the conditions of carbon deposition. *Int j hydrogen energ* 34: 4321-4330.
58. Lwin Y (2000) Chemical Equilibrium by Gibbs Energy Minimization on Spreadsheets. *Int j eng edu* 16: 335-339.
59. Gordon S, McBride BJ (1994) Computer program for calculation of complex chemical equilibrium compositions and applications: National Aeronautics and Space Administration.
60. Haynes DJ, Shekhawat D (2011) Oxidative Steam Reforming. *Fuel cells: technologies for fuel processing*: 129-190.
61. Smith MW, Shekhawat D (2011) Catalytic Partial Oxidation. *Fuel cells: technologies for fuel processing*: 73-128.
62. Nahar GA (2010) Hydrogen rich gas production by the autothermal reforming of biodiesel (FAME) for utilization in the solid-oxide fuel cells: A thermodynamic analysis. *Int j hydrogen energ* 35: 8891-8911.
63. Enger BC, Lødeng R, Holmen A (2008) A review of catalytic partial oxidation of methane to synthesis gas with emphasis on reaction mechanisms over transition metal catalysts. *Appl catal a-gen* 346: 1-27.
64. Williams MC (2011) Fuel Cells. *Fuel cells: technologies for fuel processing*: 11-27.

65. Pant K, Gupta RB (2008) Fundamentals and Use of Hydrogen as a Fuel. In: Gupta RB, editor. *Hydrogen Fuel Production, Transport, and Storage*: CRC Press.
66. Dejong M, Reinders A, Kok J, et al. (2009) Optimizing a steam-methane reformer for hydrogen production. *Int j hydrogen energ* 34: 285-292.
67. Wilhelm DJ, Simbeck DR, Karp AD, et al. (2001) Syngas production for gas-to-liquids applications technologies, issues and outlook. *Fuel process technol* 71: 139-148.
68. Aasberg-Petersen K, Bak Hansen JH, Christensen TS, et al. (2001) Technologies for large-scale gas conversion. *Appl catal a-gen* 221: 379-387.
69. Rostrup-Nielsen JR (2000) New aspects of syngas production and use. *Cataly today* 63: 159-164.
70. Enger BC, Lødeng R, A H (2008) A review of catalytic partial oxidation of methane to synthesis gas with emphasis on reaction mechanisms over transition metal catalysts. *Appl catal a-gen* 346: 1-27.
71. Kumar R, Ahmed S, Krumpelt M (1996) The low-temperature partial oxidation reforming of fuels for transportation fuel cell systems. Fuel cell seminar. Kissimmee, FL (United States), 17-20 Nov 1996: Argonne National Laboratory, Argonne, IL.
72. Vagia E, Lemonidou A (2007) Thermodynamic analysis of hydrogen production via steam reforming of selected components of aqueous bio-oil fraction. *Int j hydrogen energ* 32: 212-223.



AIMS Press

© 2016 Lifita N. Tande et al., licensee AIMS Press. This is an open access article distributed under the terms of the Creative Commons Attribution License (<http://creativecommons.org/licenses/by/4.0>)